Research Article

Dielectrical parameters and relaxation of Al/NFT/p-Si schottky diode with frequency dependence

Emine KARAGÖZ[1] , Songül FİAT VAROL*[2] , Serkan SAYIN[3], Ziya MERDAN[1]

[1]Gazi University, Faculty of Arts and Sciences, Physics Department, Ankara,06560, Türkiye
[2]Manisa Celal Bayar University, Vocational School of Technical Sciences, Electric and Energy Department, Manisa,45140, Türkiye
[3]Giresun University, Faculty of Engineering, Environmental Engineering, Giresun, 28200, Türkiye

ARTICLE INFO

ABSTRACT

The fabricated Al/ Naphthalimide /p-Si Schottky diode's dielectrical parameters and series resistance effect have been investigated by using the DC and AC measurements. W e have developed a facile interface structure that consisted of double-layer films in order to investigate the capacitance volume and series resistance effect through the device. The organic interlayer with little nanometer thickness between electrode and inorganic semiconductor drastically reduce the series resistance at the interface. The dielectric parameters have increased with decreasing frequency. Interestingly, the value of ε' (≈ 3) even at 1 kHz shows that the prepared naphthalimide (with Thiophene property) nano-interlayer can provide more charges or energy storage ability and so it can be used instead of traditional interfacial layers.

INTRODUCTION

Organic materials have been gaining a considerable attention of the scientific community due to their favorable features and unique applications. These materials can be chemically tailored to adjust separately the band gap, valance and conduction band energies [1].

During the last decade, organic semiconductors have also drew attention due to their characteristic features as an active layer for next-generation electronics due to ease in their patterning and their tunable molecular structure, flexibility, light-weight, and large-area applicability. In particular, their promising potential low cost is expected to begin an era of disposable electronics [2–7].

In recent studies, we have found some examples on metal–semiconductor (MS) structures with interfacial layers such as; Fullerene derivatives, poly[9,9-dioctylfluorenyl-2,7-diyl]-co-1,4-benzo-(2,1,3)-thiadiazole, polyvinyl alcohol,

---

*Corresponding author.
*E-mail address: emine.karagoz@yahoo.com

Bismuth Titanate, perylenetetracarboxylic dianhydride, CdS-PVA, zinc-oxide, and graphene-doped PVA structures, metal-ferroelectric-semiconductors, metal-insulator-semiconductors that attract more attention than the conventional Metal/Semiconductor structures in electronic industry [8–16]. MIS is the most suitable contact and shows the compatibleness between the insulator and semiconductor materials [17]. As reported in many studies, the conduction mechanism and formation of barrier height at M/S interface could be changed with an appropriate interlayer between semiconductor and metal [18]. The applied voltage on the diode is shared by interfacial layer, series resistance and depletion layer [17, 19].

In addition to dielectric parameters, the subject of relaxation covers all types of stress relief in solids—dielectric, mechanical, photoconductive, chemical and so on, and several of these may have points in common and so, this work will also concentrate on this issue by connecting dielectric phenomena. A wide range of scope of relaxation is also an associated with interfacial processes in metal–insulator, semiconductor–insulator, electrode–electrolyte and similar systems. Naphthalimides, due to their unique properties, have found applications in many areas of chemistry, such as fluorescent sensors, dyes, chemical probes, sensing of biologically relevant cations and anions, and also in the pharmaceutical field as anti-cancer treatments and in many other applications [20].

This paper introduces a new developmental family of thin film dielectric material covers 1,8-naphtalimide derivative that has interesting fluorescent properties and can be used as an effective tool for the monitoring and quantification of compounds.

EXPERIMENTAL DETAILS

Materials and Methods

Preperation of Organic: All starting materials and reagents were obtained as commercial sources. An analytical Thin Layer Chromatography (TLC) plates.

N-[1-(thiophene-2-yl)methyl]-1,8-napthalimide (**3**) synthesizing process steps are as follows: A flask was charged with 2-aminomethylthiophene (4.59 mmol), 1,8-naphthanoic anhydride (5.05 mmol) was refluxed in 80 mL Tetrahydrofuran. The mixture was refluxed for ~40 h. Then the volatile was evaporated to be dried. The crude was treated with water to adjust pH 6.8, and kept in an oven for dryness. The precipitation was completed by addition of a mixture of DCM/MeOH (1/25). Then, the precipitate was filtered and dried. The obtained compound with white color was synthesized with a 99.9% yield. [21].

Diode Fabrication

For the Schottky diode manufacturing, p-type Silicon (Si) wafer with orientation (100) was used as semiconductor material and Aluminium (Al) as the metallic contacts. RCA cleaning process steps applied for the p-Si surface to remove any metalic, oxide or any other chemical impurities. Al metal contact was fabricated by magnetron sputtering system under ~10^{-5} mbar pressure to evaporate the ohmic back contact over the Si substrate. For the diffusion of Al inside the Si, the wafer was heated in a tube furnace at 570 °C for 5 min under nitrogen gas flow. The top surface was cleaned again to deposit the napthalimide layer. 5 mg N-Thiophene Naphthalimide was dissolved in 2ml chloroform for 5 minutes. It was coated over the whole clean surface of p-Si substrate with a spin coater with 5000 rpm spinning speed for ~100 s. After the organic layer deposition, the substrate was held on the hotplate for 1 min at 180 °C to have a highly stacked organic layer on Si and also a for a more homogeneous and smooth interface between Si wafer and the organic dye. Al as a front point contact was deposited on the organic layer with magnetron sputtering system under 10^{-5} torr pressure. The thickness of organic layer was ~140 nm and the contacts were ~125 nm. The schematic diagram of the studied device and the molecular structure are shown in Fig. 1 (as inset in synthetic route of organic layer). Then, the Al/naphthalimide/p-Si diode was obtained. The Capacitance–Voltage (C–V) and conductance–voltage (G/w–V) measurements were carried out using a Hewlett Packard 4192A (50 Hz-13 MHz) LF impedance analyzer in the frequency range of 1kHz-5MHz at room temperature.

RESULTS AND DISCUSSION

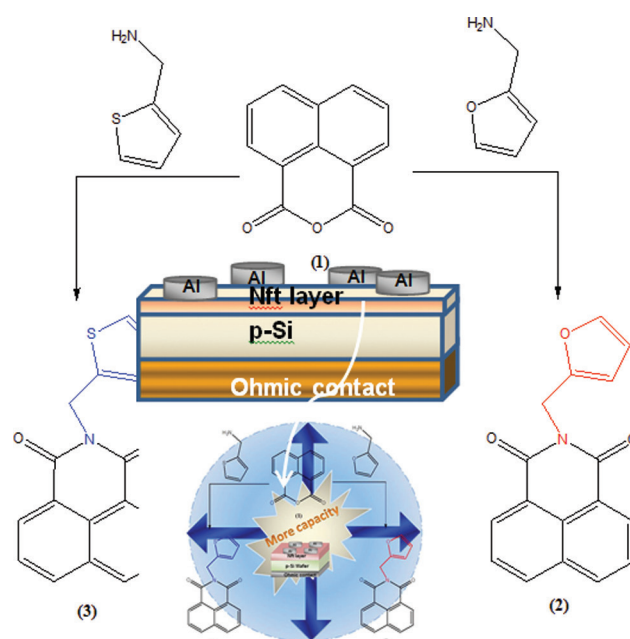The dependence of the frequency is very crucial issue for electronic tools. In real, in fact, these devices do not

Figure 1. Synthetic route for *N*-[1-(tiyofen-2-il)metil]-1,8-naphthalimide **3** [61].

depend on capacitance or are too weak, especially at high-frequency limit (f ≥1 MHz). With this, frequency dependence of the ac signal may generate a capacitance due to the interface states in excess to depletion layer. The reasons for their occurrence are the discontinuance of the periodic lattice structure at the surface, surface morphology, barrier height formation at metal–organic interface, and the distribution of the impurities of the organic layer. Under these circumstances, an excess capacitance may occur because of interface states, and it brings an increase in the real capacitance of the materials. Such changes in the existing capacitance and conductance particularly depend on the frequency and applied voltage [22–25]. In addition, interface states can easily follow the external ac signal when a low frequency applied and yield an excess capacitance also conductance, which depends on the interface states relaxation time and the ac signal frequency [26]. It must be noted that dielectric properties study concerns with the relationship between the external measured macroscopic quantities such as dielectric permittivity, electrical conductivity and the microstructure of the dielectric material [27, 28];

The frequency dependencies of dielectric constant (ε′), dielectric loss (ε″), loss tangent (tanδ) and ac electrical conductivity (σac) are investigated for Metal/Organic/Semiconductor Schottky type diode. The values of the dielectric properties were obtained from the C–V and G/w–V measurements in 1 kHz–5 MHz frequency range at room temperature. The complex permittivity can be derived from the following equation [29–31];

$$\varepsilon^* = \varepsilon' - j\varepsilon'' \tag{1}$$

The complex permittivity formalism has been employed to describe the electrical and dielectric properties. In the e* formalism, in the case of admittance measurements, the following relation holds:

$$\varepsilon^* = \frac{Y^*}{jwC_o} = \frac{C_m}{C_o} - j\frac{G}{wC_o} \tag{2}$$

where Y^*, C and G are the measured admittance, capacitance and conductance of the dielectric, and w the angular frequency ($w = 2\pi f$) of the applied electric field [31, 32].

The real part of the dielectric constant (ε′) at various frequencies is calculated using the measured capacitance values (C_m) at the strong accumulation region according to the relation [33, 34],

$$\varepsilon' = \frac{C_m}{C_o} \tag{3}$$

where C_o is capacitance of an empty capacitor. $C_o = \varepsilon_o(A/d)$; where A is the rectifier contact area in cm^{-2}, d is the interfacial layer thickness and ε_o is the permittivity of free space charge (ε_o = 8.85 x 10^{-14} F/cm). In the strong accumulation

region, the maximal capacitance of the device corresponds to the insulator capacitance (C_{ox}) ($C_{ac} = C_{ox} = \varepsilon''\varepsilon_o A/d$).

The imaginary part of the complex permittivity, the dielectric loss (ε″), at the various frequencies is calculated using the measured conductance values from the relation,

$$\varepsilon'' = \frac{G_m}{wC_o} \tag{4}$$

The loss tangent (tan δ) is the ratio of the imaginary ε″ and the real ε′ parts of the dielectric constant and is giving by [31–35],

$$\tan\delta = \frac{\varepsilon'}{\varepsilon''} \tag{5}$$

The ac electrical conductivity (σac) of the dielectric material can be given by the following equation [29, 36, 37],

$$\sigma_{ac} = wC\tan\delta(d/A) = w\varepsilon_o\varepsilon'' \tag{6}$$

Fig. 2 (a, b, c) show the dielectric constant (ε′), dielectric loss (ε″) and loss tangent (tanδ) of Al/N-T Nft/p-Si (Metal/Organic/Semiconductor) Schottky diode with the frequency dependence, respectively. From the derived capacitance and conductance values, the values of the ε′, ε″ and tand were found a strong dependence of frequency especially at low frequency values. According to these figures, ε′ and ε″ show a decrease with increasing frequency. With this increase, the contributions of the interfacial, dipolar or the ionic polarization assume an inefficient role left behind only the electronic part. This observed decrease in ε′ and ε″ with increasing frequency reflects dielectric relaxation caused by the inability of the dipolar molecules in the sample to change orientation direction with increasing rates of alteration of the applied field [38]. It means that the decreasing of ε′ and ε″ with increase in frequency is explained with increase in frequency, the interfacial dipoles have less time to orient themselves in the alternating field direction [39 – 43]. Also, this may be because the switching of the small-molecule dipoles is unable to match the switching of the electric field at high frequencies [44].

The dielectric material enhances the storage capacity of the capacitor by neutralizing the charges at the electrodes in a known manner to the external space. Dielectric or electrical insulating materials are materials that can resist electrostatic fields for a long time. When the correct voltage (dc) is applied to these substances, they show great resistance against passing of electric current, The values of ε′ and ε″ were found as 2.78, 0.57 at 1 kHz and 0.1, 0.03 at 5 MHz, respectively. Also the forming defects during the deposition process by disrupting the crystalline structure can cause the carriers in the interface to recombine without following the signal so this prevents the occur of additional capacitance.
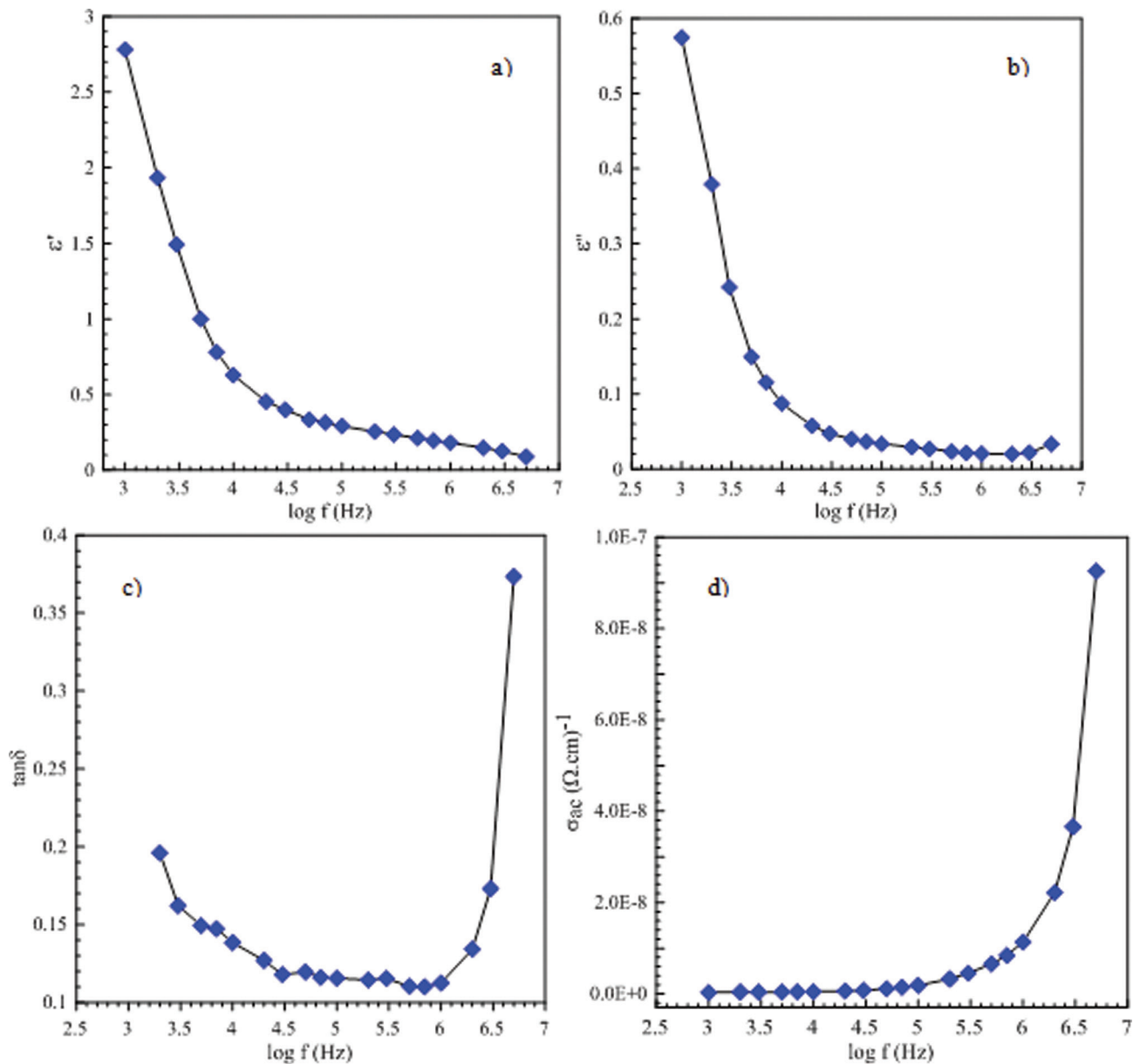
Figure 2. Frequency dependence of the a) dielectric constants (ε') b) dielectric loss (ε'') c) tangent loss (tanδ) d) the ac electrical conductivity (σ_{ac}) values at room temperature for Al/Nft/p-Si Schottky diode.

Dielectric loss factor tanδ, refers to the losses in electrical energy due to non-linear physical mechanisms such as electrical conductivity, dielectric relaxation, dielectric resonance. These losses act as a significant thermal source at high voltage or high frequency. This causes more thermal stress of the dielectric material under these conditions and lead to change its properties [45, 46]. Therefore, when selecting dielectric materials, the loss factor is it should be as small as it is.

As shown in Fig. 2(c). loss tangent, tanδ decreases with increasing frequency in the range from 1 kHz to 2 MHz, but after 2 MHz it shows a sudden rise to 0.37 at 5 MHz.

This manner in tanδ and thus increase in conductivity is achieved by an increase in the delivery of the residual current and the delivery of the absorption current [47– 49]. This shows that they are closely related to each other. The increase of the conductivity σ_{ac} is accompanied by an increase of the eddy current, which in turn increases the energy loss tanδ. With this, the electrical conductivity generally increase with increasing frequency and especially shows a sharp increase in the σ_{ac} after about 2 MHz (Fig 2d). This behavior can be attributed to the result of a decreasing series resistance with increasing frequency [50]. Also, the peak in the loss tangent can be attributed
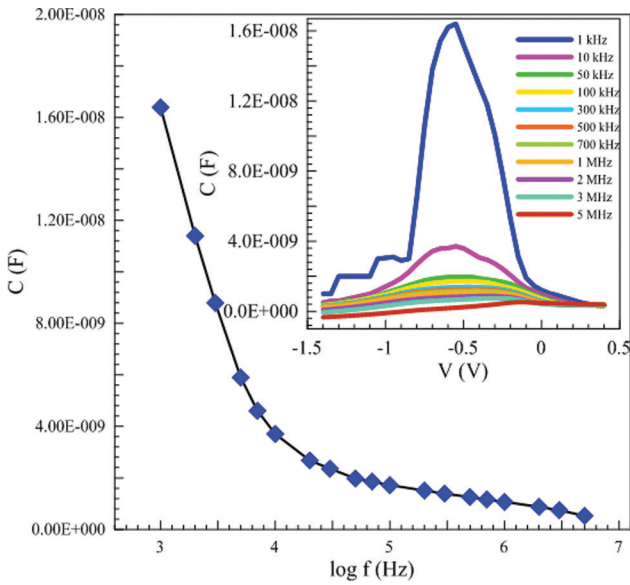
Figure 3. Variation of the capacitance (C) with frequency and voltage (V) (inset) of the Al/Nft/p-Si Schottky diode.
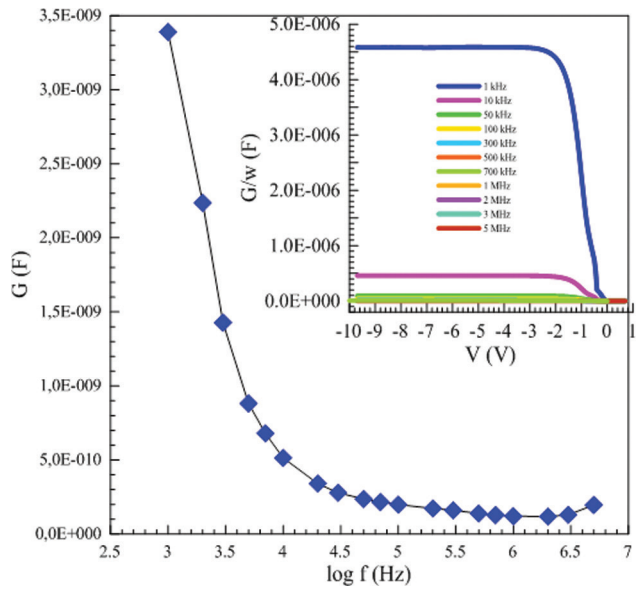

Figure 4. Variation of the conductance (G) with frequency and voltage (V) (inset) of the Al/Nft/p-Si Schottky diode.

to the Maxwell–Wagner interfacial polarization (matching of hopping frequency with frequency of external electric field) [47, 51, 52]. So, there become a gradual drop in ε′ with frequency increase. Conversely, there is a sudden drop in ε″ values with non-relaxation sign.

Fig. 3 and Fig. 4 show the capacitance (C) and conductance (G/w) plots. There is a peak with a just after the depletion region for C-V plots at low frequencies and then the capacitance shows a sudden decrease particularly after 1 kHz (Fig.3). Also the magnitude of the peak in the depletion region is gradually decreased with increasing frequency due to the time dependent response of interface states and shifts towards the positive bias region due to deep level states and series resistance. This is also due to the effect of interface state density [53–57]. The device yields much higher conductivity in the forward bias region compared to reverse bias region because the device is in the form of a Schottky type device.

Series resistance R$_s$ is one of the important sources of small signal energy loss in Schottky devices. This results in a critical error in extraction of interfacial properties and doping profiles from the admittance measurements [58, 59].

Then, the admittance Y$_{ma}$ is given by [22, 31, 60, 61]:

$$Y_{ma} = \left[G_{ma} + jwC_{ma} \right] \tag{7}$$

where the series resistance is the real part of the impedance Z$_{ma}$ =1/Y$_{ma}$. Thus, the real series resistance of MS devices can be subtracted from the obtained capacitance (C$_{ma}$) and conductance (G$_{ma}$) in strong accumulation region at high frequency values [57].

$$C_{ma} = \frac{C_{ox}}{\left(1 + w^2 R_s^2 C_{ox}^2\right)} \tag{8}$$

$$C_{ox} = C_{ma}\left[1 + \left(\frac{G_{ma}}{wC_{ma}}\right)^2\right] = \frac{\varepsilon_i \varepsilon_o A}{d_{ox}} \tag{9}$$

There are several reference works in the literature to obtain of R$_s$ values [22, 62–64]. It has been applied the method that provides the determination of R_s in both reverse and forward bias regions, presented in refs. [53, 65]. According to this method, the real R$_s$ of Schottky type diodes can be subtracted from the measured C$_m$ and G$_m$ values at sufficiently high frequency (f>500 kHz) [22, 31], using the following equation:

$$R_2 = \frac{\left(G_{ma}\right)}{G_{ma}^2 + \left(wC_{ma}\right)^2} \tag{10}$$

where *w* is the angular frequency. The G and ω symbols are conductance and angular frequency parameters (ω=2πf), respectively. The G and G/ω units are Ω^{-1} or S and Farad, respectively. Here, in order to show the G and C quantities at same unit (Farad), the values of G were divided by ω.

As seen in Fig. 5 (a, b), the series resistance gives a peak depending on frequency in the voltage range about -4.9 V for 1 kHz and -0.1 V for 5 MHz.

In Fig. 5 (a, b), the plots fluctuates in the form of 2-3 peaks, especially at low frequencies due to the particular density distribution profile of surface states. The real value of Rs was obtained as 274 Ω at 50 kHz, 20.8 Ω at 500 kHz
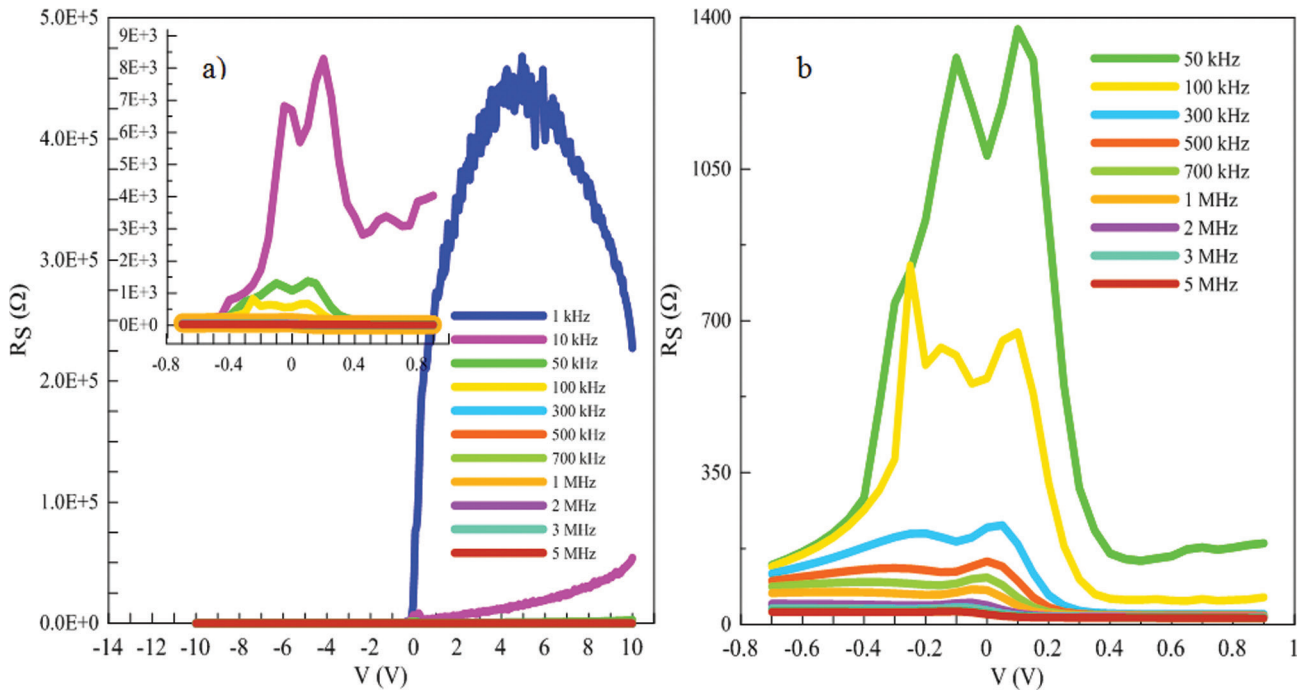
Figure 5. Al/Nft/p-Si Schottky diode's Rs-V frequency-dependent (1 kHz-5 MHz) graphics at room temperature a) Frequency-dependent graphics at 1 kHz-5 MHz interval b) Frequency-dependent graphics to see the plots better at 50 kHz-5 MHz interval.
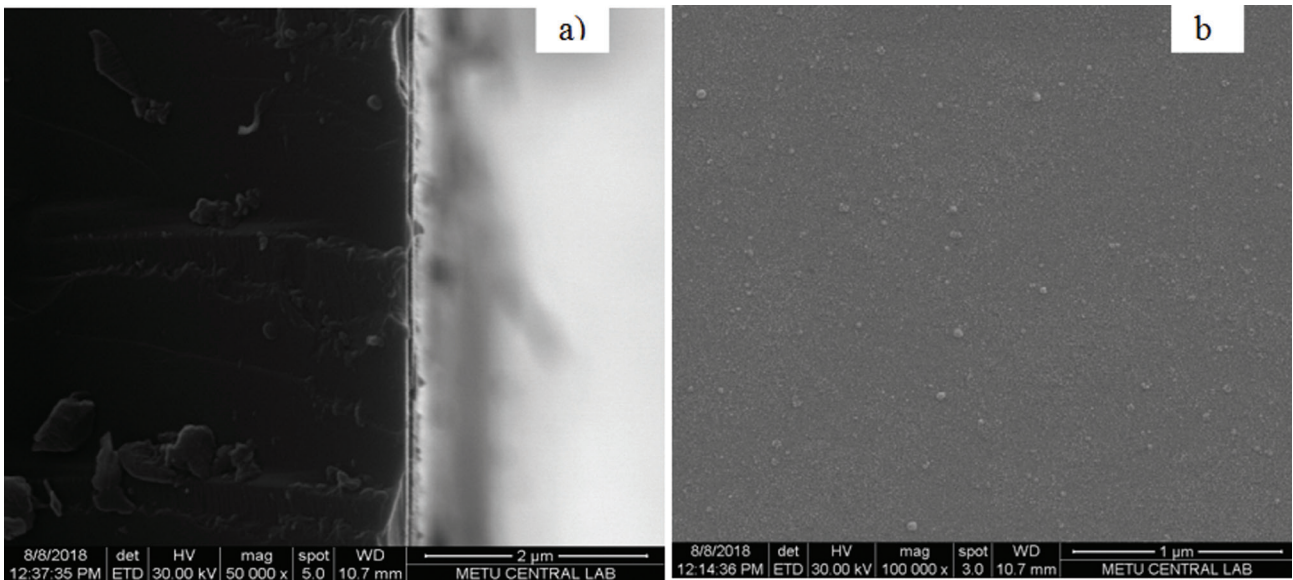

Figure 6. a) Cross-section (50 000 x), b) surface (100 000 x) of Al/Nft/p-Si Schottky barrier diodes of SEM micrographs.

and 12.8 Ω at 5MHz for 2 V and also 1370 Ω at 50 kHz, 27.3 Ω at 500 kHz and 7.37 Ω at 5 MHz for 8 V, respectively. It is clear that the resistance value is not only dependent on the frequency but also the voltage, and it decreases with increasing frequency for each bias voltage. The increase of Rs at low frequencies is originated from the existence of surface states and surface or dipole polarization, but their effect is as low as it could be ignored at sufficiently high frequencies (relatively f ≥1 MHz).

Finally, when we look at the surface map of the diode, we can see a homogeneous morphological order and grain formation (Fig. 6 (a,b)). These images show the typical

morphological pattern of the prepared Al/N-T Nft/p-Si/Al Schottky barrier diode.

Evidently, from the SEM image of the Naphthalimide content structure, it was seen that the morphology of the particles were almost spherical in shape in Fig 6(b), but agglomerated to some extent due to the interaction between nanoparticles. It can be observed that grains of uniform size are distributed throughout the surface and the formation of nanosized crystallites was confirmed through SEM images. The average grain size calculated from linear intercept method was found to be in the nanometer range of 55–76 nm.

CONCLUSIONS

The existence of naphthalimide organic layer converts metal–semiconductor (MS) devices into metal–Insulator–semiconductor (MIS) diodes and made a strong influence on the diode characteristics as well as the dielectrical properties and series resistance. The increase of σac with increasing frequency was attributed to the increase eddies current that leads to the increase in the energy tanδ. The series resistance was one of the reasons of C-V and G/ω-V curve tendency. It exhibited a meaningful decrease with increasing frequency, and the analogous trend was also seen in dielectric constant and dielectric loss such that their decrease with frequency increasing means that interface states can no longer follow a.c. signal because of the lifetime of traps is bigger than angular frequency inverse. Dielectric constant at 1 kHz is around 2.78 in the high accumulation region and decreases with increasing frequency. In addition, investigation of a.c. conductivity in the low frequency region revealed a d.c. conductivity value of 4.16×10^{-10} 1/Ωcm. We can also put a remarkable note that: while naphthalimide layer formed on a semiconductor by the traditional methods probably can passivate the active dangling bonds on the surface of semiconductor and so can decrease the amount of active dangling bonds and so leads to a decrease in the leakage current and series resistance (Rs) and maybe less effective surface states.

ACKNOWLEDGEMENTS

AUTHORSHIP CONTRIBUTIONS

Authors equally contributed to this work.

DATA AVAILABILITY STATEMENT

The authors confirm that the data that supports the findings of this study are available within the article. Raw data that support the finding of this study are available from the corresponding author, upon reasonable request.

CONFLICT OF INTEREST

The author declared no potential conflicts of interest with respect to the research, authorship, and/or publication of this article.

ETHICS

There are no ethical issues with the publication of this manuscript.

REFERENCES

[1] Gullu O, Kılıcoglu T, Turut A. Electronic properties of the metal/organic interlayer/inorganic semiconductor sandwich device J Phys Chem Solids 2010;71:351–356. [CrossRef]

[2] Voss D. Organic electronics: cheap and cheerful circuits. Nature 2000;407:442–444. [CrossRef]

[3] Berggren M, Nilsson D, Robinson ND. Organic materials for printed electronics. Nat Mater 2007;6:3–5.

[4] Lee J, Sung WJ, Joo CW, Cho H, Cho N, Lee GW, et al. Simplified bilayer white phosphorescent organic light-emitting diodes. ETRI J 2016;38:260–264. [CrossRef]

[5] Jung SW, Na BS, Baeg KJ, Kim M, Yoon SM, Kim J, et al. Nonvolatile ferroelectric P (VDF-TrFE) memory transistors based on inkjet-printed organic semiconductor. ETRI J 2013;35:734–737. [CrossRef]

[6] Kim YH, Moon DG, Han JI. Organic TFT array on a paper substrate. IEEE Electron Device Lett 2004;25:702–704. [CrossRef]

[7] Forrest SR. The path to ubiquitous and low–cost organic electronic appliances on plastic. Nature 2004;428:911–918. [CrossRef]

[8] Mustafa M, Sherin L, Kim HC, Lee YW, Choi KH. Fabrication and conduction mechanism evaluation of polyfluorene polymeric Schottky diode. Polym Adv Technol 2015;26:1109–1113. [CrossRef]

[9] Tascıoglu I, Tuzun Ozmen I, Sagban HM, Yaglıoglu E, Altındal S. Frequency dependent electrical and dielectric properties of Au/P3HT: PCBM: F4–TCNQ/n–Si Schottky Barrier Diode. J Electron Mater 2017;46:2379–2386. [CrossRef]

[10] Ersoz G, Yucedag I, A.–Kalandaragh Y, Orak I, Altındal S. Investigation of electrical characteristics in Al/CdS–PVA/p–Si (MPS) structures using impedance spectroscopy method. IEEE Trans Electron Dev 2016;63:2948–2955. [CrossRef]

[11] Demirezen S, Kaya A, Vural O, Altındal S. The effect of Mo–doped PVC+ TCNQ interfacial layer on the

electrical properties of Au/PVC+ TCNQ/p–Si structures at room temperature. Mater Sci Semicond Process 2015;33:140–148. [CrossRef]

[12] Asar YS, Asar T, Altındal S, Ozcelik S. Dielectric spectroscopy studies and ac electrical conductivity on (AuZn)/TiO2/p–GaAs (110) MIS structures. Phil Mag 2015;95:2885–2898. [CrossRef]

[13] Yeriskin SA, Balbasi M, Tataroglu A. Frequency and voltage dependence of dielectric properties, complex electric modulus, and electrical conductivity in Au/7% graphene doped–PVA/n–Si (MPS) structures. J Appl Poly Sci 2016;133. [CrossRef]

[14] Bulbul MM, Altindal S, Parlakturk F, Tataroglu A. The density of interface states and their relaxation times in Au/Bi4Ti3O12/SiO2/n-Si (MFIS) structures. Surf Interface Anal 2011;43:1561–1565. [CrossRef]

[15] Tecimer H, Uslu H, Alahmed ZA, Yakuphanoglu F, Altındal S. On the frequency and voltage dependence of admittance characteristics of Al/PTCDA/P–Si (MPS) type Schottky barrier diodes (SBDs). Compos Part B: Eng 2014;57:25–30. [CrossRef]

[16] Altindal YS, Unal HI, Bekir S. Electrical and dielectric characteristics of Al/polyindole Schottky barrier diodes. II. Frequency dependence. J Appl Poly Sci 2011;120:390–396. [CrossRef]

[17] Nikravan A, Badali Y, Altındal S, Uslu I, Orak I. On the frequency and voltage–dependent profiles of the surface states and series resistance of Au/ZnO/n–Si structures in a wide range of frequency and voltage. J Electron Mater 2017;46:5728–5736. [CrossRef]

[18] Hudait MK, Krupanidhi SB. Effects of thin oxide in metal–semiconductor and metal–insulator–semiconductor epi-GaAs Schottky diodes. Solid–State Electron 2000;44:1089–1097. [CrossRef]

[19] Divigalpitiya WMR. Temperature dependence of the photovoltaic characteristics of silicon MIS solar cells. Sol Energy Mater 1989;18:253–262. [CrossRef]

[20] Saito G, Velluto D, Resmini M. Synthesis of 1,8–naphthalimide–based probes with fluorescent switch triggered by flufenamic acid. R Soc Open Sci 2018;5:172137. [CrossRef]

[21] Karagoz E, Varol SF, Sayın S, Merdan Z. Electrical characterization of two analogous Schottky contacts produced from N–substituted 1, 8–naphthalimide. Phys Chem Chem Phys 2018;20:30502–30513. [CrossRef]

[22] Nicollian EH, Brews JR. Metal–Oxide–Semiconductor (MOS) Physics and Technology. 1st ed. New York: Wiley; 1982.

[23] Deuling H, Klausmann E, Goetzberger A. Interface states in Si☐SiO 2 interfaces. Solid State Electron, 1972;15:559–571. [CrossRef]

[24] Depas M, Van Meirhaeghe RL, Lafere WH, Cardon F. Electrical characteristics of Al/SiO2/n–Si tunnel diodes with an oxide layer grown by rapid thermal oxidation. Solid State Electron 1994;37:433–441. [CrossRef]

[25] Castange R, Vapaille A. Description of the SiO2☐Si interface properties by means of very low frequency MOS capacitance measurements. Surf Sci 1971;28:157–193. [CrossRef]

[26] Yeriskin SA, Unal HI, Sari B. Electrical and dielectric characteristics of Al/Polyindole schottky barrier diodes. II. frequency dependence J Appl Poly Sci 2010;120:390–396. [CrossRef]

[27] Asaka N, Shinyashiki N, Umehara T, Mashimo S. Dielectric dispersion of primary alcohols in polymer complex. J Chem Phys 1990;93:8273–8275. [CrossRef]

[28] Miura N, Yagihara S, Mashimo S. Microwave dielectric properties of solid and liquid foods investigated by time-domain reflectometry. J Food Sci 2003;68:1396–1403. [CrossRef]

[29] Symth CP. Dielectric Behaviour and Structure. 1st ed. New York: McGraw–Hill; 1955.

[30] Daniel VV. Dielectric Relaxation. 1st ed. London: Academic Press; 1967.

[31] Fiat S, Polat I, Bacaksiz E, Kompitsas G, Cankaya G. The influence of annealing temperature and tellurium (Te) on electrical and dielectrical properties of Al/p–CIGSeTe/Mo Schottky diodes. Curr Appl Phys 2013;13:1112–1118. [CrossRef]

[32] Tataroglu A. Electrical and dielectric properties of MIS Schottky diodes at low temperatures. Microelectron Eng 2006;83:2551–2557. [CrossRef]

[33] Popescu M, Bunget I. Physics of Solid Dielectrics. 1st ed. Amsterdam: Elsevier; 1984.

[34] Chelkowski A. Dielectric Physics. 1st ed. Amsterdam: Elsevier; 1980.

[35] Yakuphanoglu F, Yoo YT, Okutan M. An impedance spectroscopy study in poly (butylene adipate) ionomers. Ann Phys 2004;516:559–568. [CrossRef]

[36] Mattsson MS, Niklasson GA, Forsgren K, Harsta A. A frequency response and transient current study of β–Ta 2 O 5: Methods of estimating the dielectric constant, direct current conductivity, and ion mobility. J Appl Phys 1999;85:2185–2191. [CrossRef]

[37] Prabakar K, Narayandass SK, Mangalaraj D. Dielectric properties of Cd0. 6Zn0. 4Te thin films. Phys Status Solidi A 2003;199:507–514. [CrossRef]

[38] Al–Karmi AM. Impedance spectroscopy of gamma irradiated PM–355. Radiat Measur 2006;41:209–212.

[39] Maurya D, Kumar J. Dielectric–spectroscopic and ac conductivity studies on layered Na2–XKXTi3O7 (X= 0.2, 0.3, 0.4) ceramics. J Phys Chem Solids 2005;66:1614–1620. [CrossRef]

[40] Sattar AA, Rahman SA. Dielectric properties of rare earth substituted Cu–Zn ferrites. Phys Status Solidi A 2003;200:415–422. [CrossRef]

[41] Nouh SA, Gaafar SA, Eissa HM. The effect of α–particle dose on the dielectric properties of solid state nuclear track detectors. Phys Status Solidi A 1999;175:699–704. [CrossRef]

[42] Fanggao C, Saunders GA, Lambson EF, Hampton RE, Carini G, Marco GD, et al. J Appl Poly Sci 1996;34:425. [CrossRef]

[43] Ranga Raju MR, Choudhary RNP, Ram S. Dielectric and electrical properties of Sr5EuCr3Nb7O30 nanoceramics prepared using a novel chemical route. Phys Status Solidi B 2003;239:480–489. [CrossRef]

[44] L. Shi L, Yang R. Lu S, Jia K, Xiao C, Lu T, et al. Dielectric gels with ultra–high dielectric constant, low elastic modulus, and excellent transparency. NPG Asia Mater 2018;10:821–826. [CrossRef]

[45] Burtfoot JC. Ferroelectrics: An introduction to the phycical principles. 1st ed. London: Van–Nostrand–Reinbold; 1967.

[46] Sonerud B, Bengtsson T, Blennow J, Gubanski SM. Dielectric response measurements utilizing semi–square voltage waveforms. IEEE Trans Dielectr Electr Insul 2008;15:920–926. [CrossRef]

[47] Shah N, Singh NL, Desai CF, Singh KP. Microhardness and radiation damage studies of proton irradiated kapton films. Radiat Measur 2003;36:699. [CrossRef]

[48] Singh NL, Sharma A, Shrinet V, Rakshit AK, Avasthi DK. Electrical properties of ion irradiated polypropylene films. Bull Mater Sci 2004;27:263–267. [CrossRef]

[49] Tareev B. Physics of Dielectric Materials. Moscow: Mir Publication; 1975.

[50] Tataroglu A, Altındal S, Karadeniz S, Tugluoglu N. Au/SnO2/n–Si (MOS) structures response to radiation and frequency. Microelectron J 2003;34:1043–1049. [CrossRef]

[51] Singh M, Dogra A, Kumar R. Effect of 50 MeV Li3+ ion irradiation on structural, dielectric and permeability studies of In3+ substituted Mg–Mn ferrite. Nucl Instrum Methods Phys Res B 2002;196:315–323. [CrossRef]

[52] Konofaos N, Evangelou EK, Aslanoglou X, Kokkoris M, Vlastou R. Dielectric properties of CVD grown SiON thin films on Si for MOS microelectronic devices. Semicond. Sci Technol 2003;19:50. [CrossRef]

[53] Nicollian EH, Brews JR. Mos (Metal Oxide Semiconductor) Physics and Technology. 1st ed. New York: Wiley; 2002.

[54] Ho PS, Yang ES, Evans HL, Wu X. Electronic states at silicide–silicon interfaces. Phys Rev Lett 1986;56: 177.

[55] Werner J, Levi AFJ, Tung RT, Anzlowar M, Pinto M. Origin of the Excess Capacitance at Intimate Schottky Contacts. In: Mönch W, editor. Electronic structure of metal–semiconductor contacts. 1st ed. Berlin: Springer; 1990. p. 244–247. [CrossRef]

[56] Chattopadhyay P, Raychaudhuri B. New technique for the determination of series resistance of Schottky barrier diodes. Solid State Electron 1992;35:1023–1024. [CrossRef]

[57] Tataroglu B,Altındal S, Tataroglu A. The C–V–f and G/ω–V–f characteristics of Al/SiO2/p–Si (MIS) structures. Microelectron Eng 2006;83:2021–2026. [CrossRef]

[58] Karatas S. Studies on electrical and the dielectric properties in MS structures. J Non Cryst. Solids 2008;354: 3606–3611. [CrossRef]

[59] Maiti CK, Dalapati GK, Chatterjee S, Samanta SK, Varma S, Patil S. Electrical properties of high permittivity ZrO2 gate dielectrics on strained–Si..Solid State Electron 2004;48:2235–2241. [CrossRef]

[60] Nicollian EH, Goetzberger A. The si–sio, interface–electrical properties as determined by the metal–insulator–silicon conductance technique. Bell Syst Tech J 1967;46:1033–1055. [CrossRef]

[61] Hung KK, Cheng YC. Characterization of Si-SiO2 interface traps in p-metal-oxide-semiconductor structures with thin oxides by conductance technique. J Appl Phys 1987;62:4204–4211. [CrossRef]

[62] Norde H. A modified forward I-V plot for Schottky diodes with high series resistance. J Appl Phys 1979;50:5052–5053. [CrossRef]

[63] Sato K, Yasamura Y. Study of forward I-V plot for Schottky diodes with high series resistance. J Appl Phys 1985;58:3655–3657. [CrossRef]

[64] Cheung SK, Cheung NW. Extraction of Schottky diode parameters from forward current-voltage characteristics. Apply Phys Lett 1986;49:85–87. [CrossRef]

[65] Nicollian EH, Brews JR. Instrumentation and analog implementation of the QC method for MOS measurements. Solid State Electron 1984;27:953–962. [CrossRef]